Quantum Fisher information from randomized measurements

Aniket Rath, Cyril Branciard, Anna Minguzzi, Benoît Vermersch

Quantum Fisher Information from Randomized Measurements

Aniket Rath,[1] Cyril Branciard,[2] Anna Minguzzi,[1] and Benoît Vermersch[1,3,4]
[1]Université Grenoble Alpes, CNRS, LPMMC, 38000 Grenoble, France
[2]Université Grenoble Alpes, CNRS, Grenoble INP, Institut Néel, 38000 Grenoble, France
[3]Center for Quantum Physics, University of Innsbruck, Innsbruck A-6020, Austria
[4]Institute for Quantum Optics and Quantum Information of the Austrian Academy of Sciences, Innsbruck A-6020, Austria

(Received 7 June 2021; accepted 17 November 2021; published 22 December 2021)

The quantum Fisher information (QFI) is a fundamental quantity of interest in many areas from quantum metrology to quantum information theory. It can in particular be used as a witness to establish the degree of multiparticle entanglement in quantum many-body systems. In this work, we use polynomials of the density matrix to construct monotonically increasing lower bounds that converge to the QFI. Using randomized measurements we propose a protocol to accurately estimate these lower bounds in state-of-the-art quantum technological platforms. We estimate the number of measurements needed to achieve a given accuracy and confidence level in the bounds, and present two examples of applications of the method in quantum systems made of coupled qubits and collective spins.

DOI: 10.1103/PhysRevLett.127.260501

First introduced in quantum metrology to measure the ability for quantum states to perform interferometry beyond the shot-noise limit [1,2], the quantum Fisher information (QFI) plays a fundamental role in different fields, including quantum information theory and many-body physics. As enhanced sensitivity for metrology and sensing requires the generation of multipartite entangled states [3], the QFI has raised significant interest as a witness of entanglement. In particular, the notion of entanglement "depth"—the minimum number of entangled particles in a given state—and the underlying structure of multipartite entanglement can be related to the value of the QFI [4,5]. In many-body physics, the ability for the QFI to reveal the entanglement of mixed states makes it a key quantity in the study of spin models, revealing in particular universal entanglement properties of quantum states crossing a phase transition at finite temperature [6] and highlighting the role of multipartite entanglement in topological phase transitions [7]. This Letter presents a protocol to estimate the QFI in state-of-the-art quantum devices via randomized measurements.

The challenge to measure the QFI arises from it being a highly nonlinear function of the density matrix. The QFI is defined with respect to a given Hermitian operator A and a quantum state ρ, and can be written in the following closed form:

$$F_Q = 2\mathrm{Tr}\left(\frac{(\rho\otimes\mathbb{1}-\mathbb{1}\otimes\rho)^2}{\rho\otimes\mathbb{1}+\mathbb{1}\otimes\rho}\mathbb{S}(A\otimes A)\right), \qquad (1)$$

where $\mathbb{S}$ is the swap operator defined through its action on basis states $|i_1\rangle$, $|i_2\rangle$ by $\mathbb{S}(|i_1\rangle\otimes|i_2\rangle)=|i_2\rangle\otimes|i_1\rangle$. We clarify the form of Eq. (1)—noting that the fraction notation is allowed by the fact that the numerator and denominator commute—and relate it to the standard expression of the QFI: $F_Q=2\sum_{(i,j),\lambda_i+\lambda_j>0}[(\lambda_i-\lambda_j)^2/(\lambda_i+\lambda_j)]|\langle i|A|j\rangle|^2$, with $\rho=\sum_i\lambda_i|i\rangle\langle i|$, in the Supplemental Material [8]. For pure states $\rho=|\psi\rangle\langle\psi|$, the QFI is proportional to the variance of the operator A, $F_Q=4(\langle\psi|A^2|\psi\rangle-\langle\psi|A|\psi\rangle^2)$. According to the quantum Cramér-Rao relation, the QFI bounds the achievable precision in parameter estimation in quantum metrology [4]. Furthermore, for N spins $1/2$, with a collective spin operator $A=\frac{1}{2}\sum_{l=1}^{N}\sigma_\mu^{(l)}$ [12], all separable states satisfy $F_Q\leq N$ [3]. This means that, if $F_Q>N$, the state is entangled, and provides an advantage over all separable states for performing quantum metrology.

The QFI can also be used to certify multipartite entanglement in terms of k-producibility, i.e., a decomposition into a statistical mixture of tensor products of k-particle states, or m-separability, i.e., a decomposition into a statistical mixture of products of at least m factors, of the state ρ [5,13,14]. In particular, the inequality $F_Q>\Gamma(N,k)$, with $\Gamma(N,k)=\lfloor N/k\rfloor k^2+(N-\lfloor N/k\rfloor k)^2$, implies that a state is not k-producible, i.e., that it has an entanglement depth of at least $k+1$. Note that one can show the QFI being above a certain threshold value by measuring a *lower bound* of it. This includes quantities associated with the expectation value of an observable, such as spin squeezing [3,15–19], or multiple quantum coherence [20]. Recently, nonlinear lower bounds to the QFI, not accessible by standard observable measurements, have also been introduced [21–26] and measured [27]. However, the finite distance between these bounds and the QFI typically limits the ability to certify quantum states for metrology, or to detect multipartite entanglement. If the quantum state is in a thermal state, the QFI can also be

measured via dynamical susceptibilities [28]. However, the states used in the context of quantum metrology [4], and many-body dynamics [29], are usually out of equilibrium.

Here, we propose a systematic and state-agnostic way to estimate the QFI by measuring a converging series of monotonically increasing approximations F_n, $F_0 \leq F_1 \leq \ldots \leq F_Q$, which rapidly tend to F_Q as n increases. Thus, each F_n, being a lower-bound to the QFI, allows the verification of quantum metrological advantage and/or multipartite entanglement of the quantum state ρ. Moreover, each function F_n, being a *polynomial* function of the density matrix ρ, can be accessed by randomized measurements. Such protocols only require single qubit random rotations and measurements and have been successfully applied to obtain Rényi entropies [30–34], negativities [11,35–37], state overlaps [38] (which lead to the sub-QFI, a lower bound on the QFI measured in Ref. [27]), scrambling [39,40], and topological invariants [41,42]. Note that multipartite entanglement conditions can also be expressed as statistical moments of randomized measurements [43–47].

Construction of converging lower bounds.—We define the bounds F_n as

$$F_n = 2\mathrm{Tr}\left(\sum_{\ell=0}^{n}(\rho\otimes\mathbb{1}-\mathbb{1}\otimes\rho)^2(\mathbb{1}\otimes\mathbb{1}-\rho\otimes\mathbb{1}-\mathbb{1}\otimes\rho)^{\ell} \times \mathbb{S}(A\otimes A)\right). \quad (2)$$

The construction of the above bounds is detailed in the Supplemental Material [8], where we show that $\forall\ n \in \mathbb{N}$, $F_n \leq F_Q$, and $F_n \leq F_{n+1}$ with the inequalities saturating for pure and fully mixed states. For the first two bounds, we obtain

$$F_0 = 4\mathrm{Tr}(\rho[\rho, A]A), \quad (3)$$

$$F_1 = 2F_0 - 4\mathrm{Tr}(\rho^2[\rho, A]A). \quad (4)$$

where [,] is the commutator. As shown in the Supplemental Material [8], the constructed series F_n converges exponentially with n to F_Q. Note that the quantity F_0 was shown to be a lower bound of the QFI in Refs. [21–24], while the sub-QFI of Refs. [26,27] is a lower bound to F_0. We remark that F_0 was proven to be faithful to the QFI with respect to global extrema [26].

Figure 1(a) illustrates this convergence for different purities of the noisy GHZ state $\rho(p) = (1-p)|\mathrm{GHZ}_N\rangle\langle\mathrm{GHZ}_N| + p\mathbb{1}/2^N$ with $|\mathrm{GHZ}_N\rangle = (|0\rangle^{\otimes N} + |1\rangle^{\otimes N})/\sqrt{2}$, and $A = \frac{1}{2}\sum_{l=1}^{N}\sigma_z^{(l)}$ (where to maximize the QFI obtained for this state, we choose the direction $\mu = z$ for A). GHZ states of up to 20 qubits have been realized in recent quantum platforms [48–50]. This class of states can be used to achieve

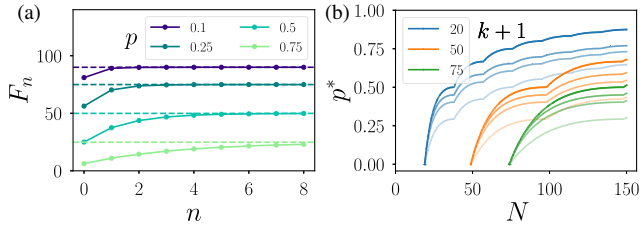

FIG. 1. Convergence of the lower bounds and entanglement depth certification. Panel (a) shows the QFI (dashed lines) and its lower bounds F_n as a function of the order n (dots connected by solid lines) for a 10-qubit GHZ state mixed with different white noise strengths p (see legend). The convergence nature of F_n is commented on in the Supplemental Material [8]. Panel (b) shows for noisy GHZ states, the threshold value of white noise p^* as a function of the number of qubits N to detect different entanglement depths of (at least) $k+1$ (see legend) by F_0, F_1, F_2, and F_Q (light to dark).

enhanced sensitivities in quantum metrology [4] as they exhibit nontrivial multipartite entanglement, which cannot be detected using spin-squeezing inequalities [4]. One of the important consequences of having a series of monotonically increasing bounds is that one detects multipartite entanglement more efficiently as n increases. This is illustrated in Fig. 1(b), where for various values of N and k, we consider the maximal value p^*, such that an entanglement depth of at least $k+1$ is detected via the inequality $F_n > \Gamma(N,k)$ [which implies $F_Q > \Gamma(N,k)$]. The noise tolerance p^* increases as a function of the order n of the lower bounds and is upper bounded by the p^* value corresponding to F_Q.

Randomized measurement protocol.—Let us now show how the bounds F_n can be accessed from randomized measurements. Such protocols first gave access to the purity $\mathrm{Tr}(\rho^2)$ [31], and then later to any polynomial of the density matrix [10,11,33,36]. What makes our bounds F_n accessible from randomized measurements data is precisely that they are polynomials of ρ (of order $n+2$).

A schematic of the protocol is shown in Fig. 2(a). For concreteness, we first consider a system of N qubits, and discuss the case of collective spin systems further below. In our protocol, the N-qubit quantum state ρ is prepared in the experiment and we apply local random unitaries u_i sampled from the circular unitary ensemble (CUE) (or a unitary 2-design [51]). We record as a bit string $s = s_1, \ldots, s_N$ the outcomes of a measurement in a fixed computational basis. This sequence is repeated for M distinct unitaries $u = u_1 \otimes \cdots \otimes u_N$, for which classical bit strings $s^{(r)}$ with $r = 1, \ldots, M$ are stored [52].

From this data, we have enough information to reconstruct the density matrix in the limit $M \to \infty$ [53–55]. To access directly the function F_n, we use the classical shadow formalism [10], and assign to each recorded bit-string $s^{(r)} = s_1^{(r)}, \ldots, s_N^{(r)}$ an operator

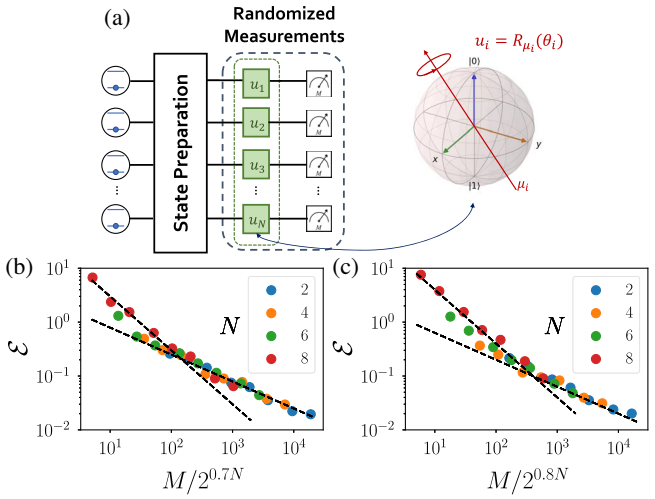

FIG. 2. Protocol and statistical error scaling. Panel (a) illustrates the randomized measurement protocol needed to estimate the lower bounds of the QFI. Local random unitaries are applied followed by measurements performed in a fixed computational basis. Panels (b) and (c) show the error scaling for F_0 and F_1, respectively, by considering a GHZ state mixed with a depolarization noise of strength $p = 0.25$, and for various values of N (see legends). The dashed black lines highlight the different error scalings $\propto 1/M$ and $1/\sqrt{M}$.

$$\hat{\rho}^{(r)} = \bigotimes_{l=1}^{N} [3(u_l^{(r)})^\dagger |s_l^{(r)}\rangle\langle s_l^{(r)}| u_l^{(r)} - \mathbb{1}_2]. \tag{5}$$

The operator $\hat{\rho}^{(r)}$ is known as a "classical shadow" in the sense that the average over the unitaries and the bit-string measurement results gives $\mathbb{E}[\hat{\rho}^{(r)}] = \rho$. For different independently sampled shadows labeled r, r', we obtain similarly that $\hat{\rho}^{(r)}\hat{\rho}^{(r')}$ are unbiased estimations of ρ^2 [10]. This approach using U-statistics [9] generalizes to estimate any power ρ^j, by using j different shadows $\hat{\rho}^{(r_1)}, \ldots, \hat{\rho}^{(r_j)}$. Then by linearity, we write the unbiased estimator $\hat{F}_n$ of F_n using combinations of $M \geq n+2$ different shadows $\rho^{(r)}$. In particular, for $n = 0$, 1, from Eqs. (3)–(4) we obtain the following unbiased estimators for F_0 and F_1, respectively:

$$\hat{F}_0 = \frac{4}{2!}\binom{M}{2}^{-1} \sum_{r_1 \neq r_2} \mathrm{Tr}(\hat{\rho}^{(r_1)}[\hat{\rho}^{(r_2)}, A]A), \tag{6}$$

$$\hat{F}_1 = 2\hat{F}_0 - \frac{4}{3!}\binom{M}{3}^{-1} \sum_{r_1 \neq r_2 \neq r_3} \mathrm{Tr}(\hat{\rho}^{(r_1)}\hat{\rho}^{(r_2)}[\hat{\rho}^{(r_3)}, A]A). \tag{7}$$

Notice that, using independent measurements, the experimental setting of randomized measurements remains the same as in quantum state tomography (QST). To measure a N-qubit quantum state ρ of rank χ using QST with $\epsilon-$ accuracy in terms of trace distance, requires $M = O(\chi^2 2^N/\epsilon^2)$ measurements [56]. Meanwhile for randomized measurements that give access to polynomial functions of ρ, the number of measurements to overcome statistical errors scale as 2^{aN} with $a \sim 1$ [31,38,39]. Furthermore, in tomography the classical postprocessing of the measurement data is expensive, as it is based on storing and manipulating exponentially large matrices. In contrast, the use of classical shadows in randomized measurements, which have a tensor product structure, cf. Eq. (5), leads to cheap estimation algorithms in postprocessing run-time and memory usage [10,11].

Statistical errors.—Statistical errors associated with the estimation of F_n arise due to the application of a finite number M of random unitary transformations. In particular, as n increases, while the bound F_n becomes tighter the degree of the polynomial in ρ of $\hat{F}_n$, evaluated with M different shadows, increases. In order to provide rigorous performance guarantees for our protocol, we analytically study the probabilities $\Pr[|\hat{F}_n - F_n| \geq \epsilon]$ that the statistical errors are larger than a certain accuracy ϵ. Using the Chebyshev's inequality $\Pr[|\hat{F}_n - F_n| \geq \epsilon] \leq \mathrm{Var}[\hat{F}_n]/\epsilon^2$, we relate these to the variance $\mathrm{Var}[\hat{F}_n]$ of our estimations. As shown in the Supplemental Material [8], we provide an upper bound to $\mathrm{Var}[\hat{F}_n]$ by generalizing the results of Ref. [10,11] to arbitrary density matrix polynomials. This allows us to calculate for any N-qubit quantum state ρ the required number of measurements M to estimate $\hat{F}_n$ within a certain confidence interval, so that $\Pr[|\hat{F}_n - F_n| \geq \epsilon] \leq \delta$ for a given δ. Our results show that the required value of M scales as $\alpha 2^N$ with respect to N, where α can be calculated for any order n based on the knowledge of the state ρ and the operator A [8]. As an illustration, we calculate in particular the value of α for pure GHZ states, and in the limit of high accuracy $\epsilon \to 0$. We find that, while F_0 can be evaluated with fewer measurements compared to F_1, there is an overall scaling of 2^N for both required values of M.

To complement our analytical study, we numerically study the error scalings for F_0 and F_1 by simulating the experimental protocol. The average statistical error $\mathcal{E}$ is computed by averaging over 50 simulated experimental runs the relative error $\hat{\mathcal{E}} = |\hat{F}_n - F_n|/F_n$ of the estimated bound $\hat{F}_n$. We consider the N-qubit noisy GHZ state with $A = \frac{1}{2}\sum_{l=1}^{N} \sigma_z^{(l)}$. Figures 2(b),2(c) show the scaling of the average statistical error in estimating F_0 and F_1, as a function of rescaled number of measurements $M/2^{aN}$ with a being adjusted by collapsing the data obtained for different N onto a single curve. The figures show that the required number of measurements to obtain an error accuracy of 0.1 scales overall as $\sim 2^{0.7N}$ and $\sim 2^{0.8N}$ for F_0 and F_1, respectively. In particular, for large M we observe a $1/\sqrt{M}$ scaling, which is the standard error decay obtained by performing an empirical Monte Carlo average. In the regime of smaller M, the statistical error being high, decays

much faster as $1/M$. These two error regimes are also apparent in the expression of the variance (see Supplemental Material [8]). Second, as expected from the analytical expressions and seen above from the scaling exponents of F_0 and F_1, we observe that estimating F_1 requires slightly more measurements compared to F_0 (see also Supplemental Material [8] for nonrescaled data). Note that similar error scalings, and transition from $1/\sqrt{M}$ to $1/M$ behaviors have been observed for other types of cubic order terms related to entanglement negativities [11,35]. In addition, importance sampling approaches can be incorporated in randomized measurement protocols, leading to change of scaling exponents governing statistical errors, and thus drastic reductions of the required number of measurements [57–60].

Systematic errors.—Present quantum devices are vulnerable to systematic errors due to noise [61]. However, the effect of noise occurring during a measurement can be mitigated. First, in the presence of depolarization or qubit readout errors, estimation formulas from randomized measurements can be corrected to provide unbiased estimations [34,38,62,63]. Furthermore, in the classical shadows formalism, robust estimations can be performed in the presence of an *unknown* noise channel. This is achieved via a calibration step, which uses a state that can be prepared with high fidelity [64–66]. Under the assumption of gate-independent Markovian noise, the data obtained from such calibration provide a model to build robust classical shadows from randomized measurements. In the presence of gate-dependent noise, this framework can also be used, showing as well error mitigation [64–66]. These techniques can be applied readily in our protocol.

Protocol for collective spin systems.—We now extend our approach to an ensemble of N particles described by a collective spin $S = (N/2)$. These systems implemented with ultracold atoms or trapped ions, are relevant to quantum metrology [15–18,28] as they can feature large-scale multipartite entanglement [19]. Remarkably, our protocol provides access to the series F_n in these systems with relatively low numbers of measurements M.

Consider for concreteness a set of N ultracold bosons in a double-well potential, as illustrated in Fig. 3(a). It is convenient to write the state of the system in terms of $N+1$ Fock states $|n_1, n_2\rangle$ or $|n_1 - n_2\rangle$ with $n_1 \in 0, \ldots, N$, the number of atoms in the left well and $n_2 = N - n_1$ atoms in the right well. The Bose-Hubbard Hamiltonian H_t describing this system reads

$$H_t = \frac{\mathcal{J}}{2}(\hat{a}_L^\dagger \hat{a}_R + \text{H.c}) + \frac{U_{\text{int}}}{2}\sum_{\ell=L,R}\hat{n}_\ell(\hat{n}_\ell - 1) + \Delta_t(\hat{n}_L - \hat{n}_R), \tag{8}$$

where, $\hat{n}_{L,R} = \hat{a}_{L,R}^\dagger \hat{a}_{L,R}$ are the number operators given in terms of creation $\hat{a}_{L,R}^\dagger$ and annihilation $\hat{a}_{L,R}$ operators, $\mathcal{J}$ is the tunneling matrix element, U_{int} is the on-site interaction energy, and Δ_t is a random energy offset, cf. Fig. 3(a). It can be equivalently written using spin $S = (N/2)$ operators [67–69]. The random unitaries U can be experimentally generated as $U = e^{-iH_\eta T}\cdots e^{-iH_1 T}$ by choosing different random energy difference Δ_η in H_η for some time interval T. The convergence of such unitaries U to unitary 2-designs (which are required in order to build classical shadows) as a function of the depth η has been studied in Refs. [31,62,70–72]. Note that these unitaries U, considered here for randomized measurements, can also be used to generate metrologically useful quantum states [73].

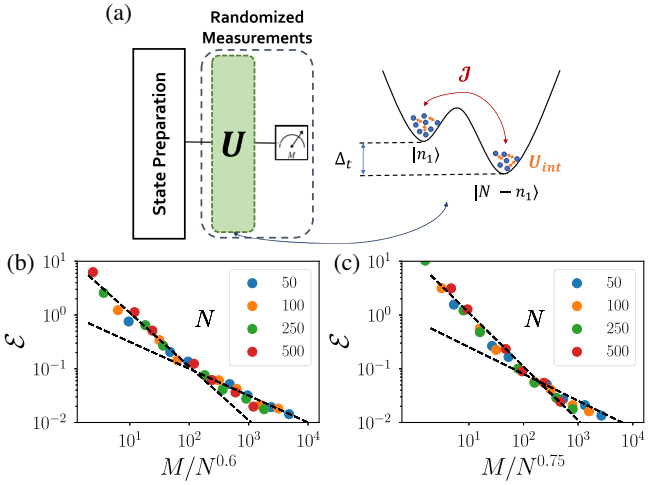

FIG. 3. Protocol and error scalings for collective spin models. Panel (a) illustrates the two-site collective spin model followed by the randomized measurement protocol implementing global random unitaries. The lower panels show the statistical error scalings of (b) F_0 and (c) F_1 for a N00N state of bosonic ensembles mixed with depolarization noise of strength $p = 0.25$ as a function of rescaled axis M/N^a, and for various values of N (see legends).

Compared to the situation of N qubits, the protocol to measure the series F_n in this system differs only in applying global random unitaries U instead of local random unitaries u. We first prepare a state ρ of interest in this system, then generate and apply random unitaries U followed by measurements of the populations (n_1, n_2) in each well. Repeating this procedure for M unitary matrices $U^{(r)}$, we collect measurement results $s^{(r)} = n_1^{(r)} - n_2^{(r)}$ with $r = 1, \ldots, M$. A classical shadow $\hat{\rho}^{(r)}$ of ρ [10,41,53] is constructed from each measurement outcome $s^{(r)}$ and the applied unitary $U^{(r)}$ as

$$\hat{\rho}^{(r)} = [(N+2)(U^{(r)})^\dagger |s^{(r)}\rangle\langle s^{(r)}| U^{(r)} - \mathbb{1}_{N+1}]. \tag{9}$$

Here, the classical shadow is a matrix of dimension $(N+1)\times(N+1)$. From this, we build our series of estimators $\hat{F}_n$ from the measurement data in the same way as shown earlier for the N-qubit systems.

We investigate the statistical error scalings to estimate the lower bounds F_0 and F_1 by computing the average relative error $\mathcal{E}$. Consider the N00N state given by $|\mathrm{N00N}\rangle = (1/\sqrt{2})(|N,0\rangle + |0,N\rangle)$ [4]. Such states provide optimal metrological sensitivities and are genuinely multipartite entangled, i.e., they have an entanglement depth of N [4]. The observable A is taken to be the population difference between the two wells and is defined as $A = \hat{n}_1 - \hat{n}_2$. We numerically analyze the scaling of statistical errors by directly generating global random unitaries from the CUE. For simplicity, we study a state $\rho(p) = (1-p)|\mathrm{N00N}\rangle\langle\mathrm{N00N}| + p\mathbb{1}/(N+1)$ subject to depolarization noise of strength $p = 0.25$. Various other noise models have been studied for macroscopic superposition states in Refs. [74–77]. In the case of an *a priori* unknown noise channel, one can use again the formalism of robust shadows to correct our estimates of F_n [64–66]. Figures 3(b),3(c) show that the required number of measurements here no longer scale exponentially but subpolynomially in the number of atoms N for F_0 and F_1. This is attributed to the fact that the Hilbert space dimension scales linearly in N. The required number of measurements for obtaining an error of 0.1 is found to scale as N^{a_0} and N^{a_1} with $a_0 \sim 0.6$ and $a_1 \sim 0.75$ for F_0 and F_1, respectively.

Conclusion and outlook.—Our method to access the QFI can be used for asserting states capable of providing enhanced metrological sensitivities, or in the context of entanglement detection and quantum simulation. Importantly, we can make predictions on the required number of measurements to detect entanglement with a certain confidence interval. As a future direction, it would be interesting to compare the entanglement detection "power" of different protocols based on randomized measurements. This includes in particular approaches based on the positive partial transpose condition [11,27,36], which can be applied in the multipartite case [78], and on statistical correlations of Pauli measurements [43–47].

We thank A. Elben and R. Kueng for fruitful discussions, and comments on the manuscript. B. V. thanks P. Zoller for inspiring discussions and previous collaborations on randomized measurements. A. R. is supported by Laboratoire d'excellence LANEF in Grenoble (ANR-10-LABX-51-01) and from the Grenoble Nanoscience Foundation. B. V. acknowledges funding from the Austrian Science Fundation (FWF, P 32597 N). B. V. and A. M. acknowledge funding from the French National Research Agency (ANR-20-CE47-0005, JCJC project QRand). For our numerical simulations we used the quantum toolbox QuTiP [79].

[1] S. L. Braunstein and C. M. Caves, Phys. Rev. Lett. **72**, 3439 (1994).
[2] S. L. Braunstein, C. M. Caves, and G. J. Milburn, Ann. Phys. (N.Y.) **247**, 135 (1996).
[3] L. Pezzé and A. Smerzi, Phys. Rev. Lett. **102**, 100401 (2009).
[4] L. Pezzè, A. Smerzi, M. K. Oberthaler, R. Schmied, and P. Treutlein, Rev. Mod. Phys. **90**, 035005 (2018).
[5] Z. Ren, W. Li, A. Smerzi, and M. Gessner, Phys. Rev. Lett. **126**, 080502 (2021).
[6] P. Zanardi, M. G. A. Paris, and L. C. Venuti, Phys. Rev. A **78**, 042105 (2008).
[7] L. Pezzè, M. Gabbrielli, L. Lepori, and A. Smerzi, Phys. Rev. Lett. **119**, 250401 (2017).
[8] See Supplemental Material at http://link.aps.org/supplemental/10.1103/PhysRevLett.127.260501 for further details on the derivation of our bounds, a convergence analysis, and analytical study of statistical errors, which includes Refs. [1,2,9,10,11].
[9] W. Hoeffding, in *Breakthroughs in Statistics* (Springer, New York, 1992), pp. 308–334.
[10] H.-Y. Huang, R. Kueng, and J. Preskill, Nat. Phys. **16**, 1050 (2020).
[11] A. Elben, R. Kueng, H.-Y. R. Huang, R. van Bijnen, C. Kokail, M. Dalmonte, P. Calabrese, B. Kraus, J. Preskill, P. Zoller, and B. Vermersch, Phys. Rev. Lett. **125**, 200501 (2020).
[12] $\sigma_\mu^{(l)}$ is the Pauli matrix in an arbitrary direction μ acting on the lth spin.
[13] G. Tóth, Phys. Rev. A **85**, 022322 (2012).
[14] P. Hyllus, W. Laskowski, R. Krischek, C. Schwemmer, W. Wieczorek, H. Weinfurter, L. Pezzé, and A. Smerzi, Phys. Rev. A **85**, 022321 (2012).
[15] T. Monz, P. Schindler, J. T. Barreiro, M. Chwalla, D. Nigg, W. A. Coish, M. Harlander, W. Hänsel, M. Hennrich, and R. Blatt, Phys. Rev. Lett. **106**, 130506 (2011).
[16] H. Strobel, W. Muessel, D. Linnemann, T. Zibold, D. B. Hume, L. Pezzè, A. Smerzi, and M. K. Oberthaler, Science **345**, 424 (2014).
[17] G. Barontini, L. Hohmann, F. Haas, J. Estève, and J. Reichel, Science **349**, 1317 (2015).
[18] J. G. Bohnet, B. C. Sawyer, J. W. Britton, M. L. Wall, A. M. Rey, M. Foss-Feig, and J. J. Bollinger, Science **352**, 1297 (2016).
[19] R. Schmied, J. D. Bancal, B. Allard, M. Fadel, V. Scarani, P. Treutlein, and N. Sangouard, Science **352**, 441 (2016).
[20] M. Gärttner, P. Hauke, and A. M. Rey, Phys. Rev. Lett. **120**, 040402 (2018).
[21] A. Rivas and A. Luis, Phys. Rev. A **77**, 063813 (2008).
[22] A. Rivas and A. Luis, Phys. Rev. Lett. **105**, 010403 (2010).
[23] C. Zhang, B. Yadin, Z.-B. Hou, H. Cao, B.-H. Liu, Y.-F. Huang, R. Maity, V. Vedral, C.-F. Li, G.-C. Guo, and D. Girolami, Phys. Rev. A **96**, 042327 (2017).
[24] D. Girolami and B. Yadin, Entropy **19**, 124 (2017).
[25] J. L. Beckey, M. Cerezo, A. Sone, and P. J. Coles, arXiv:2010.10488.
[26] M. Cerezo, A. Sone, J. L. Beckey, and P. J. Coles, Quantum Sci. Technol. **6**, 035008 (2021).
[27] M. Yu, D. Li, J. Wang, Y. Chu, P. Yang, M. Gong, N. Goldman, and J. Cai, Phys. Rev. Research **3**, 043122 (2021).
[28] M. Gärttner, J. G. Bohnet, A. Safavi-Naini, M. L. Wall, J. J. Bollinger, and A. M. Rey, Nat. Phys. **13**, 781 (2017).
[29] R. J. Lewis-Swan, A. Safavi-Naini, A. M. Kaufman, and A. M. Rey, Nat. Rev. Phys. **1**, 627 (2019).

[30] S. J. van Enk and C. W. J. Beenakker, Phys. Rev. Lett. **108**, 110503 (2012).

[31] A. Elben, B. Vermersch, M. Dalmonte, J. I. Cirac, and P. Zoller, Phys. Rev. Lett. **120**, 050406 (2018).

[32] T. Brydges, A. Elben, P. Jurcevic, B. Vermersch, C. Maier, B. P. Lanyon, P. Zoller, R. Blatt, and C. F. Roos, Science **364**, 260 (2019).

[33] V. Vitale, A. Elben, R. Kueng, A. Neven, J. Carrasco, B. Kraus, P. Zoller, P. Calabrese, B. Vermersch, and M. Dalmonte, arXiv:2101.07814.

[34] K. J. Satzinger *et al.*, arXiv:2104.01180.

[35] Y. Zhou, P. Zeng, and Z. Liu, Phys. Rev. Lett. **125**, 200502 (2020).

[36] A. Neven, J. Carrasco, V. Vitale, C. Kokail, A. Elben, M. Dalmonte, P. Calabrese, P. Zoller, B. Vermersch, R. Kueng, and B. Kraus, npj Quantum Inf. **7**, 152 (2021).

[37] X.-D. Yu, S. Imai, and O. Gühne, Phys. Rev. Lett. **127**, 060504 (2021).

[38] A. Elben, B. Vermersch, R. Van Bijnen, C. Kokail, T. Brydges, C. Maier, M. K. Joshi, R. Blatt, C. F. Roos, and P. Zoller, Phys. Rev. Lett. **124**, 010504 (2020).

[39] B. Vermersch, A. Elben, L. M. Sieberer, N. Y. Yao, and P. Zoller, Phys. Rev. X **9**, 021061 (2019).

[40] M. K. Joshi, A. Elben, B. Vermersch, T. Brydges, C. Maier, P. Zoller, R. Blatt, and C. F. Roos, Phys. Rev. Lett. **124**, 240505 (2020).

[41] A. Elben, J. Yu, G. Zhu, M. Hafezi, F. Pollmann, P. Zoller, and B. Vermersch, Sci. Adv. **6**, 3666 (2020).

[42] Z.-P. Cian, H. Dehghani, A. Elben, B. Vermersch, G. Zhu, M. Barkeshli, P. Zoller, and M. Hafezi, Phys. Rev. Lett. **126**, 050501 (2021).

[43] L. Knips, J. Dziewior, W. Kłobus, W. Laskowski, T. Paterek, P. J. Shadbolt, H. Weinfurter, and J. D. A. Meinecke, npj Quantum Inf. **6**, 51 (2020).

[44] A. Ketterer, N. Wyderka, and O. Gühne, Phys. Rev. Lett. **122**, 120505 (2019).

[45] A. Ketterer, N. Wyderka, and O. Gühne, Quantum **4**, 325 (2020).

[46] A. Ketterer, S. Imai, N. Wyderka, and O. Gühne, arXiv: 2012.12176.

[47] S. Imai, N. Wyderka, A. Ketterer, and O. Gühne, Phys. Rev. Lett. **126**, 150501 (2021).

[48] K. X. Wei, I. Lauer, S. Srinivasan, N. Sundaresan, D. T. McClure, D. Toyli, D. C. McKay, J. M. Gambetta, and S. Sheldon, Phys. Rev. A **101**, 032343 (2020).

[49] C. Song, K. Xu, H. Li, Y.-R. Zhang, X. Zhang, W. Liu, Q. Guo, Z. Wang, W. Ren, J. Hao, H. Feng, H. Fan, D. Zheng, D.-W. Wang, H. Wang, and S.-Y. Zhu, Science **365**, 574 (2019).

[50] A. Omran, H. Levine, A. Keesling, G. Semeghini, T. T. Wang, S. Ebadi, H. Bernien, A. S. Zibrov, H. Pichler, S. Choi, J. Cui, M. Rossignolo, P. Rembold, S. Montangero, T. Calarco, M. Endres, M. Greiner, V. Vuletić, and M. D. Lukin, Science **365**, 570 (2019).

[51] D. Gross, K. Audenaert, and J. Eisert, J. Math. Phys. (N.Y.) **48**, 052104 (2007).

[52] Note that, to simplify the experimental procedure, it is also possible to write estimators from randomized measurements based on collecting several bit strings for each random unitary [11].

[53] M. Ohliger, V. Nesme, and J. Eisert, New J. Phys. **15**, 015024 (2013).

[54] A. Elben, B. Vermersch, C. F. Roos, and P. Zoller, Phys. Rev. A **99**, 052323 (2019).

[55] M. Guţă, J. Kahn, R. Kueng, and J. A. Tropp, J. Phys. A **53**, 204001 (2020).

[56] J. Haah, A. W. Harrow, Z. Ji, X. Wu, and N. Yu, IEEE Trans. Inf. Theory **63**, 5628 (2017).

[57] C. Hadfield, S. Bravyi, R. Raymond, and A. Mezzacapo, arXiv:2006.15788.

[58] A. Rath, R. van Bijnen, A. Elben, P. Zoller, and B. Vermersch, Phys. Rev. Lett. **127**, 200503 (2021).

[59] H.-Y. Huang, R. Kueng, and J. Preskill, Phys. Rev. Lett. **127**, 030503 (2021).

[60] S. Hillmich, C. Hadfield, R. Raymond, A. Mezzacap, and R. Wille, arXiv:2105.06932.

[61] J. Preskill, Quantum **2**, 79 (2018).

[62] B. Vermersch, A. Elben, M. Dalmonte, J. I. Cirac, and P. Zoller, Phys. Rev. A **97**, 023604 (2018).

[63] J. Vovrosh, K. E. Khosla, S. Greenaway, C. Self, M. S. Kim, and J. Knolle, Phys. Rev. E **104**, 035309 (2021).

[64] S. Chen, W. Yu, P. Zeng, and S. T. Flammia, PRX Quantum **2**, 030348 (2021).

[65] D. E. Koh and S. Grewal, arXiv:2011.11580.

[66] E. van den Berg, Z. K. Minev, and K. Temme, arXiv:2012 .09738.

[67] F. T. Arecchi, E. Courtens, R. Gilmore, and H. Thomas, Phys. Rev. A **6**, 2211 (1972).

[68] G. J. Milburn, J. Corney, E. M. Wright, and D. F. Walls, Phys. Rev. A **55**, 4318 (1997).

[69] G. Ferrini, A. Minguzzi, and F. W. J. Hekking, Phys. Rev. A **78**, 023606 (2008).

[70] C. Dankert, R. Cleve, J. Emerson, and E. Livine, Phys. Rev. A **80**, 012304 (2009).

[71] L. Banchi, D. Burgarth, and M. J. Kastoryano, Phys. Rev. X **7**, 041015 (2017).

[72] L. M. Sieberer, T. Olsacher, A. Elben, M. Heyl, P. Hauke, F. Haake, and P. Zoller, npj Quantum Inf. **5**, 78 (2019).

[73] M. Oszmaniec, R. Augusiak, C. Gogolin, J. Kołodyński, A. Acín, and M. Lewenstein, Phys. Rev. X **6**, 041044 (2016).

[74] Y. P. Huang and M. G. Moore, Phys. Rev. A **73**, 023606 (2006).

[75] G. Ferrini, D. Spehner, A. Minguzzi, and F. W. J. Hekking, Phys. Rev. A **82**, 033621 (2010).

[76] K. Pawlowski, D. Spehner, A. Minguzzi, and G. Ferrini, Phys. Rev. A **88**, 013606 (2013).

[77] K. Pawłowski, M. Fadel, P. Treutlein, Y. Castin, and A. Sinatra, Phys. Rev. A **95**, 063609 (2017).

[78] B. Jungnitsch, T. Moroder, and O. Gühne, Phys. Rev. Lett. **106**, 190502 (2011).

[79] J. Johansson, P. Nation, and F. Nori, Comput. Phys. Commun. **184**, 1234 (2013).